Available online at www.sciencedirect.com
SCIENCE DIRECT®
Surface and Coatings Technology 174–175 (2003) 1206–1210
SURFACE & COATINGS TECHNOLOGY
www.elsevier.com/locate/surfcoat

Plasma nitriding behavior of low carbon binary alloy steels

Kazuhiro Nakata[a,*], Wataru Yamauchi[b], Katsuya Akamatsu[b], Masao Ushio[a]

[a]*Joining and Welding Research Institute, Osaka University, 11-1, Mihogaoka, Ibaraki, Osaka 567-0047, Japan*
[b]*Department of Materials Science and Engineering, Kansai University, 3-3-35, Yamate, Suita, Osaka 564-8680, Japan*

Abstract

Effect of alloying elements, Cr, Ta, Ti and V with the content of 0.5, 1.0 and 1.5 mass% on plasma nitriding behavior at 823 K of nitriding temperature was examined in low carbon binary alloy steels. Deep diffusion layer with high hardness up to HV900 below the surface thin compound (γ'-Fe_4N) layer was formed in these alloys. The hardness increased with increasing alloying content. Optical microscope and X-ray diffraction (XRD) analyses did not reveal the formation of any nitride of these alloying elements in the diffusion layer. Transmission electron microscope revealed the evidence of coherent pre-precipitation phase. In XRD analysis, broadening and shift of diffraction peak of α-Fe as a matrix of the diffusion layer were observed. The peak broadening and the peak shift had a good correlation with the hardness and the nitrogen content in the diffusion layer, respectively. Accordingly, these results suggested that the hardening in the diffusion layer was caused by the microstrain in the matrix induced by the formation of coherent pre-precipitation phase.

Keywords: Plasma nitriding; Steel; Alloying element; Microstructure; Hardness; X-ray diffraction

1. Introduction

Plasma nitriding, assisted by glow discharge plasma, is one of the surface hardening processes widely used for improving wear properties of steel and alloy parts due to its beneficial features such as good reproducibility and low distortion of the treated parts, low energy and labor saving, and no requirement for anti-pollution equipment.

As the effect of the alloying element in alloy steels on the hardening behavior by plasma nitriding, Al, Cr, Mn, Mo, Nb, Si, Ti and V as the alloying element have been examined so far, and among them Al, Cr, Nb, Ti and V were the effective element on the hardness increase in the diffusion layer for steel [1–4]. Phillips and Seybolt [1] observed the formation of G.P. zone in the diffusion layer by electron transmission microscope (TEM) and suggested its effect to the hardening. The other studies discussed only the relationship between the hardness profiles and the microstructure by optical microscope (OM). In addition, these studies are on the limited alloying element or alloying content. Thus, systematic study by changing alloying content on various alloying elements has not been done yet.

In this research, 12 tentative binary alloy steels with four kinds of alloying element at three content levels for each were made to make clear the effect of alloying element and content on the hardening behavior in the plasma nitriding, and to recognize the hardening mechanism assisted with macroscopic analysis by X-ray diffraction (XRD) and microscopic analysis by OM and TEM.

2. Experimental

2.1. Materials used

Twelve kinds of low carbon binary alloy steels were tentatively made. As alloying element, Cr, Ta, Ti and V were selected with the content of approximately 0.5, 1.0 and 1.5 mass% at 0.02 mass% C level for each alloying element. These elements are well known as a strong nitride former. Other elements were controlled at less than 0.01 mass%. Cast materials were hot-rolled to the plate in 5 mm thickness and annealed at 1183 K for 3.6 ks. In addition, plain carbon steel (SPCC) with 0.02 mass% C was used for comparison.

*Corresponding author. Tel.: +81-6-6879-8656; fax: +81-6-6879-8689.
E-mail address: nakata@jwri.osaka-u.ac.jp (K. Nakata).

0257-8972/03/$ - see front matter © 2003 Elsevier Science B.V. All rights reserved.
doi:10.1016/S0257-8972(03)00459-6

2.2. Methods

Plasma nitriding treatment was performed by a d.c. glow discharge plasma nitriding unit with 28 kW in maximum power. Plasma nitriding condition is 823 K of nitriding temperature for 10.8 ks of nitriding time in a mixture gas of nitrogen and hydrogen with 50 vol.% each at total pressure 800 Pa. Specimen temperature was measured by optical pyrometer. Specimen size is $20\times35\times5$ mm^3. As a pretreatment, specimen surface was ground by SiC grinding paper #1200 and then degreased with acetone. Microstructural analysis by OM and TEM for determining the structure of nitrided layer, electron probe microanalysis (EPMA) for measuring nitrogen concentration, XRD analysis (Cu Kα, 40 kV, 150 mA, sampling width: 0.02°) for identifying the nitride and estimating the lattice distortion of the diffusion layer, and microhardness test for getting the hardness profile were carried out to the nitrided specimen.

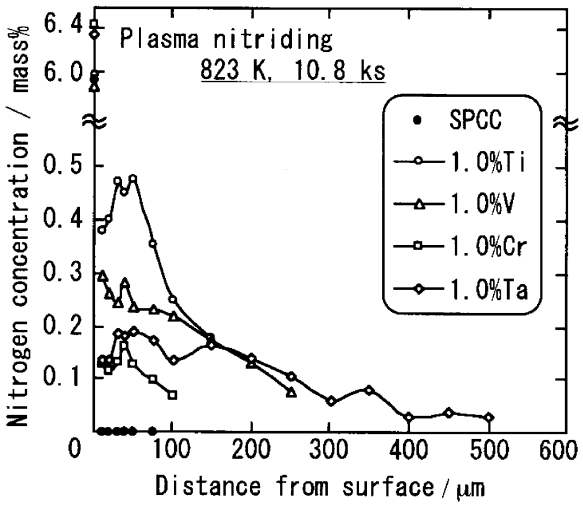

Fig. 2. Nitrogen concentration distribution on cross-section of plasma nitrided layer for SPCC and alloy steels containing 1% alloying content for each measured by EPMA.

3. Results and discussion

3.1. Microstructure

Typical microstructures of nitrided layer on the cross-section of the nitrided specimen are collectively shown in Fig. 1, which were etched with 5% nital. Single compound layer consisted of γ′-Fe_4N was formed on all the specimens, which were identified by XRD. This layer was very thin, less than 10 μm, and the difference in the layer thickness of each alloy was little. Below this top compound layer, needle like precipitates were formed selectively in the specimen of SPCC and Ta containing alloys and 0.5% Cr alloy. These precipitates were probably γ′-Fe_4N and α″-$Fe_{16}N_2$ [5,6] precipitated in the nitrogen diffusion layer during furnace cooling after plasma nitriding. However, in the other alloys there was no precipitate observed beneath the top layer, though cracking was observed in Ti containing alloys.

Fig. 2 shows the nitrogen distribution measured by EPMA on the cross-section of the nitrided specimen with 1% alloying content. Nitrogen concentration in the surface compound layer corresponds to that of γ′-Fe_4N of 5.66–5.90 mass% [7]. Next to the compound layer a deep nitrogen diffusion layer existed in all the alloy specimens. Especially in 1% Ti, 1% V and 1% Cr alloys

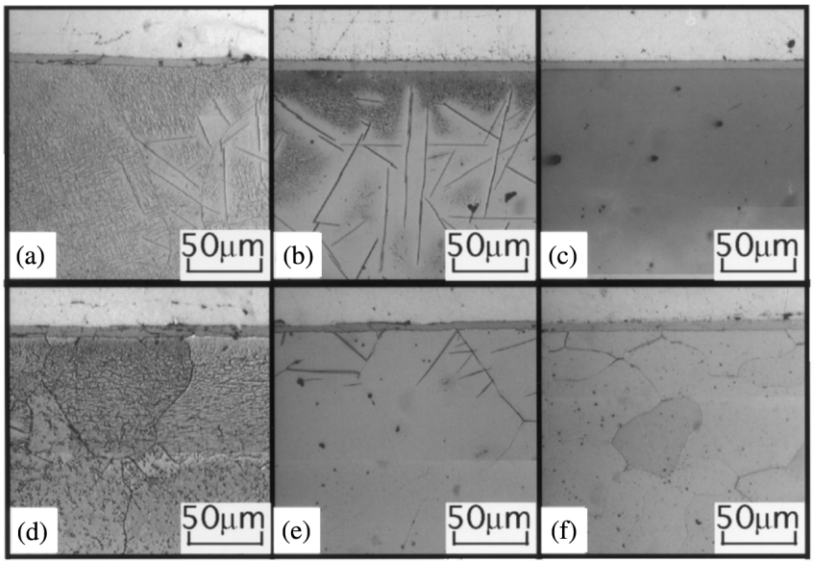

Fig. 1. Microstructures on cross-section of plasma nitrided layer nitrided at 823 K for 10.8 ks: (a) SPCC; (b) 0.5% Cr; (c) 1% Cr; (d) 1% Ta; (e) 1% Ti and (f) 1% V alloy steels.

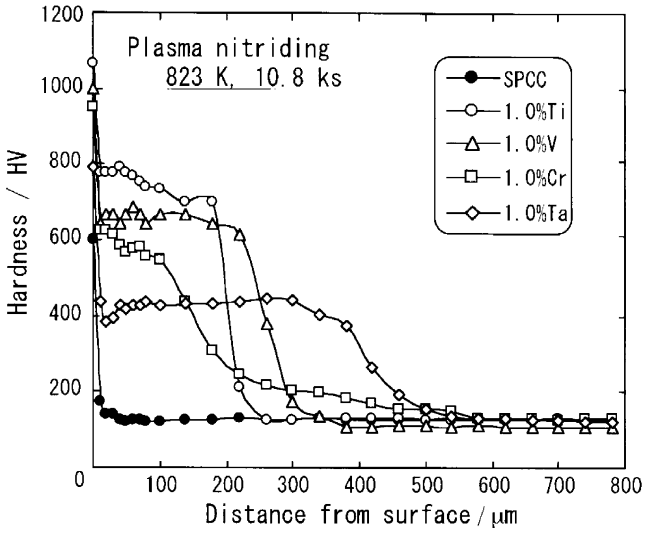

Fig. 3. Hardness profiles on cross-section of plasma nitrided layer for SPCC and alloy steels containing 1% alloying content.

showed high nitrogen concentration in spite of no nitride precipitation. On the contrary, in SPCC no detectable nitrogen concentration was measured in the diffusion layer irrespective of many needle iron nitrides. This is probably due to small volume fraction of needle nitrides due to very low nitrogen solubility in α-Fe even at the nitriding temperature. The diffusion layer of 1% Ta alloy has both features of those of SPCC and other alloys. Therefore, these differences in the microstructure was caused by the nitrogen solubility in each alloy steel.

3.2. Hardness

Fig. 3 shows typical hardness profiles on the cross-section of the nitrided specimen with 1% alloying content, treated at 823 K for 10.8 ks. Surface compound layer showed high hardness approximately HV1000 irrespective of alloying element. In SPCC, the diffusion layer showed no hardening in spite of many needle nitrides. On the contrary, alloys showed remarkable hardening with large depth and hardness plateau in the diffusion layer. Especially in 1% Cr, 1% V and 1% Ti alloys the hardness reached HV500–800 in spite of no nitride precipitation as shown in Fig. 1. One percent Ta alloy has the similar microstructure as SPCC, but also showed the obvious increase in the hardness, though its hardness is lower than those of other alloys. These hardness profiles suggest that the internal nitriding occurred in the diffusion layer of the alloys [2].

Figs. 4 and 5 show the effect of alloying content of each alloying element on the hardness and the depth of the diffusion layer, respectively. As a representative value, the hardness at the depth of 100 μm in the hardness profile in Fig. 3 was selected, and the depth meant the width of the hardened zone in comparison

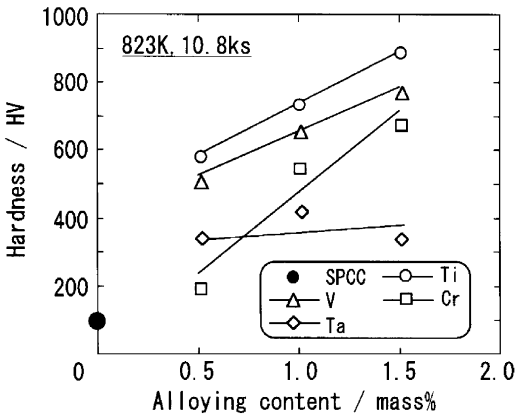

Fig. 4. Effect of alloying content on hardness of diffusion layer at the depth of 100 μm.

with the core hardness. The alloying content showed the positive effect on the hardness, but the negative to the depth in each alloy. Similar reverse relationship between the hardness and the depth was observed in the different alloying elements as Ti bearing alloy showed the highest hardness, but the smallest depth. As a nitride former, negative value of Gibbs free energy for the formation of nitride is in the order of Ti > V > Cr > Ta > Fe at the nitriding temperature. This means that the strong nitride former is easy to trap the diffused nitrogen, and thus causes high hardness and narrow depth in the diffusion layer.

3.3. Hardening mechanism

Fig. 6 shows TEM bright field images for the alloys with 1% alloying content. Many fine particles were observed. However, any nitride of these alloying elements was not detected by electron diffraction analysis. Only α-Fe phase was identified by electron diffraction spots in Fig. 6 as the matrix of the diffusion layer. High resolution TEM revealed that these particles were not

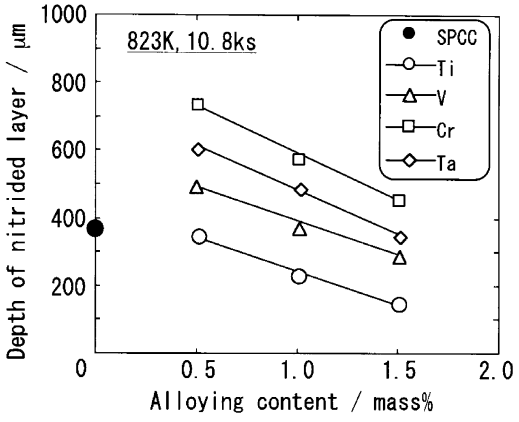

Fig. 5. Effect of alloying content on depth of nitrided layer.

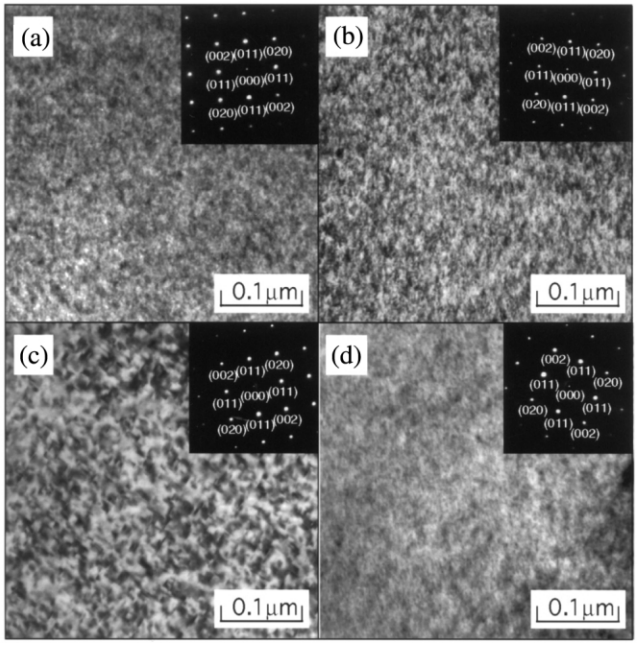

Fig. 6. TEM micrographs of diffusion layer at the depth of 100 μm: (a)1% Ti; (b)1% V; (c) 1% Cr and (d)1% Ta alloy steels, plasma nitrided at 823 K for 10.8 ks.

precipitates, but contrast images caused probably by G.P. zones or the segregation of alloying element and/or nitrogen. These pre-precipitation phases inherently possess the coherency with the matrix, and this causes the microstrain in the matrix [8]. Similar microstructure was observed in the nitrided specimens of iron alloys [1,5,9], nickel alloy [10] and molybdenum alloy [11].

XRD analysis of the diffusion layer at the depth of 100 μm showed the peak broadening and the peak shift to the low angle side as shown in Fig. 7, which showed α-Fe (1 1 0) peaks comparing before and after nitriding for the alloys with 1% alloying content and SPCC. On the contrary, in SPCC no change was observed. The degrees of the peak broadening and the peak shift were different in alloying element and content.

Increasing alloying content increased the peak shift for each alloying element. Peak shift means the uniform expansion of the lattice caused by increasing the amount of solute nitrogen as shown in Fig. 8, which shows the relation between the nitrogen concentration measured in Fig. 2 at the depth of 100 μm and the peak shift measured in Fig. 7. Therefore, it is clear that these alloying elements act to increase the amount of solute nitrogen in the diffusion layer [12].

It is well known that the microstrain in the lattice causes the peak broadening, and also causes the hardening. Fig. 9 shows the relation between the peak broadening and the hardness of the diffusion layer. The peak broadening, $\Delta 2\theta (= W_a - W_b)$ is the difference of the half value width of the (1 1 0) peaks, and W_b and

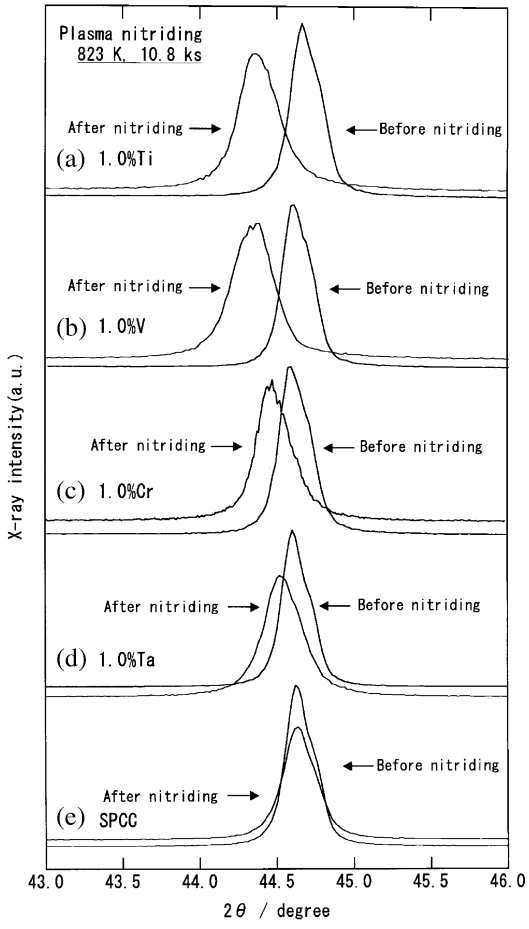

Fig. 7. XRD peaks of α-Fe (1 1 0) in diffusion layer measured at the depth of 100 μm comparing before and after plasma nitriding.

W_a are the half value widths of each peak measured before and after nitriding, respectively. The hardness increased linearly with increasing the peak broadening in each alloy. These increases in peak broadening corresponded to the increase in alloying content in each

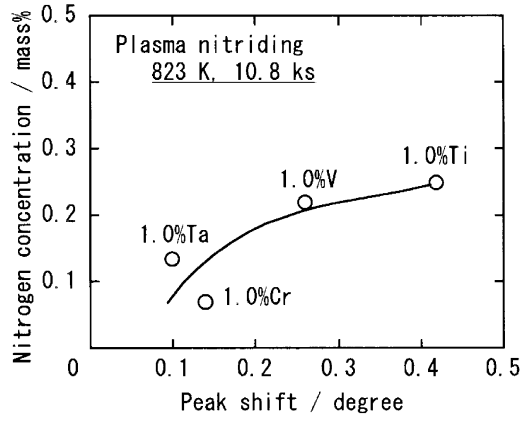

Fig. 8. Relation between nitrogen concentration of diffusion layer and peak shift of α-Fe (1 1 0) peak measured at the depth of 100 μm.

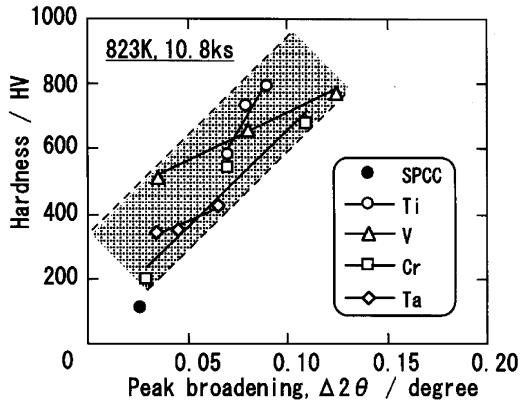

Fig. 9. Relation between hardness of diffusion layer and peak broadening of α-Fe (1 1 0) peak measured at the depth of 100 μm.

alloy. These results mean that alloying element traps diffused nitrogen and forms the pre-precipitation phase having the coherency with the matrix, thus induced the microstrain in the matrix lattice, which caused the remarkable hardening of the alloys.

4. Conclusions

Effect of alloying elements, Cr, Ta, Ti and V with the content of 0.5, 1.0 and 1.5 mass% on plasma nitriding behavior at 823 K of nitriding temperature for 10.8 ks was examined in low carbon binary alloy steels and plain carbon steel (SPCC). Main conclusions obtained are as follows;

1. The nitrided layer consisted of the surface thin γ′-Fe_4N compound layer with less than 10 μm and the second deep diffusion layer with up to 700 μm.
2. The hardness of the diffusion layer was HV400–900 depending on the alloying element and content, and increased with increasing alloying content for each alloy. In SPCC the diffusion layer was not hardened.
3. OM and XRD analyses did not reveal the formation of any nitride of the alloying element in the diffusion layer. Transmission electron microscope revealed the evidence of the pre-precipitation phase as contrast image.
4. In XRD analysis, the diffraction peak of α-Fe as a matrix of the diffusion layer broadened and shifted to lower diffraction angle. The peak broadening and the peak shift had a good correlation with the hardness and the nitrogen content in the diffusion layer, respectively.
5. These results suggested that hardening in the diffusion layer of the alloy steels was caused by the microstrain in the matrix induced by the formation of coherent pre-precipitation phase.

Acknowledgments

The authors would like to express their thanks to Dr H. Morimoto, Joining steel research Lab., Nippon Steel Cop. for offering materials.

References

[1] A.V. Phillips, A.U. Seybolt, Trans. AIME 242 (1968) 2415.
[2] A.U. Seybolt, Trans. AIME 245 (1969) 769.
[3] T. Takase, et al., J. Jpn. Inst. Metals 40 (1976) 663.
[4] R. Urao, et al., J. Surf. Finishing Soc. Jpn. 41 (1990) 106.
[5] X. Xu, et al., Metall. Mater. Trans., Part A 27 (1996) 1347.
[6] T. Sone, E. Tsunasawa, K. Yamanaka, NETSU SYORI 24 (1984) 316.
[7] T.B. Massalski, Binary Alloy Phase Diagrams, vol. 2, second ed., ASM International, 1990, p. 1728.
[8] E.J. Mittemeijer, J. Metals 7 (1985) 16.
[9] D.S. Richerby, A. Hendry, K.H. Jack, Heat Treat. 81 (1981) 130.
[10] T. Makishi, K. Nakata, Stainless Steel 2000, in: T. Bell, K. Akamatsu, (Eds.), The Insti. Materials, 2001, 133.
[11] J.B. Mitchell, Acta Metall. 19 (1971) 1063.
[12] M.A.J. Somers, R.M. Lankreijer, E.J. Mittemeijer, Philos. Mag. A 59 (1989) 353.